

Ligand Redox Effects in the Synthesis, Electronic Structure, and Reactivity of an Alkyl–Alkyl Cross-Coupling Catalyst

Gavin D. Jones,[†] Jason L. Martin,[†] Chris McFarland,[†] Olivia R. Allen,[†]
Ryan E. Hall,[†] Aireal D. Haley,[†] R. Jacob Brandon,[†] Tatyana Konovalova,[‡]
Patrick J. Desrochers,[§] Peter Pulay,[†] and David A. Vicic^{*†}

Contribution from the Department of Chemistry and Biochemistry, University of Arkansas, Fayetteville, Arkansas 72701, Department of Chemistry, University of Alabama, Box 870336, Tuscaloosa, Alabama 35487-0336, and Department of Chemistry, University of Central Arkansas, Conway, Arkansas 72035

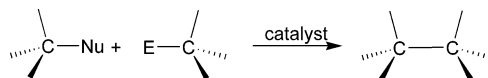
Received May 12, 2006; E-mail: dvicic@uark.edu

Abstract: The ability of the terpyridine ligand to stabilize alkyl complexes of nickel has been central in obtaining a fundamental understanding of the key processes involved in alkyl–alkyl cross-coupling reactions. Here, mechanistic studies using isotopically labeled (TMEDA)NiMe₂ (TMEDA = *N,N,N',N'*-tetramethylethylenediamine) have shown that an important catalyst in alkyl–alkyl cross-coupling reactions, (tpy')NiMe (**2b**, tpy' = 4,4',4''-tri-*tert*-butylterpyridine), is not produced via a mechanism that involves the formation of methyl radicals. Instead, it is proposed that (terpyridine)NiMe complexes arise via a comproportionation reaction between a Ni(II)–dimethyl species and a Ni(0) fragment in solution upon addition of a terpyridine ligand to (TMEDA)NiMe₂. EPR and DFT studies on the paramagnetic (terpyridine)NiMe (**2a**) both suggest that the unpaired electron resides heavily on the terpyridine ligand and that the proper electronic description of this nickel complex is a Ni(II)–methyl cation bound to a reduced terpyridine ligand. Thus, an important consequence of these results is that alkyl halide reduction by (terpyridine)NiR_{alkyl} complexes appears to be substantially ligand based. A comprehensive survey investigating the catalytic reactivity of related ligand derivatives suggests that electronic factors only moderately influence reactivity in the terpyridine-based catalysis and that the most dramatic effects arise from steric and solubility factors.

Introduction

Although the metal-catalyzed cross-coupling of an alkyl nucleophile and an alkyl electrophile (Scheme 1) is perhaps the most versatile conceivable method for forming a new C(sp³)–C(sp³) bond in an organic molecule, a number of fundamental obstacles have hindered the implementation of this method in synthetic chemistry. First, it is well-known that transition-metal alkyls are prone to β -hydride elimination reactions. Therefore, any catalytic process involving activation of alkyl nucleophiles and/or alkyl electrophiles must take into account this undesired side reaction. Strategies to suppress the β -hydride elimination reaction typically involve the use of ligands that never permit the formation of a metal–alkyl intermediate that has a fully vacant d-orbital or the use of ligands that produce a metal–alkyl intermediate that, regardless of electron count, cannot attain the requisite geometry for β -hydride elimination. These strategies are often difficult to realize, as the nature of the metal coordination sphere under catalytic conditions is not always controllable nor predictable. Second, common alkyl electrophiles, such as alkyl halides, are well-known to oxidize low valent transition metals by single-electron processes, leading to the formation of alkyl radicals and X[−]. The rates of

Scheme 1. Metal-Catalyzed Cross-Coupling of Alkyl Nucleophile with an Alkyl Electrophile



Nu = Li, MgX, ZnX, AlX₂, BR₂, etc.
E = halide, sulfonate, etc.

dimerization and other side reactions of the resulting alkyl radicals must then not be faster than the radical addition to substrate or transition metal, or efficient cross-coupling catalysis will not proceed. Moreover, the ease of alkyl halide reduction to produce alkyl radicals has serious consequences that need to be addressed when designing asymmetric versions of the alkyl–alkyl cross-coupling reactions described in Scheme 1.

Despite the considerations mentioned above, much progress has been made in recent years in identifying ligands and reaction conditions that can effectively promote alkyl–alkyl cross-couplings.¹ In 2003, Fu reported a nickel-catalyzed reaction using the pybox ligand (eq 1, pybox = bis(oxazolonyl)pyridine) that successfully achieved Negishi couplings of unactivated secondary alkyl bromides.^{1g} Conditions were then found to exploit the C₂ symmetry of the pybox ligand, as Fu later reported the first examples of asymmetric Negishi cross-couplings of alkyl electrophiles (eqs 2 and 3).^{1m,2} These experiments were seminal, as they showed that *racemic* starting materials could

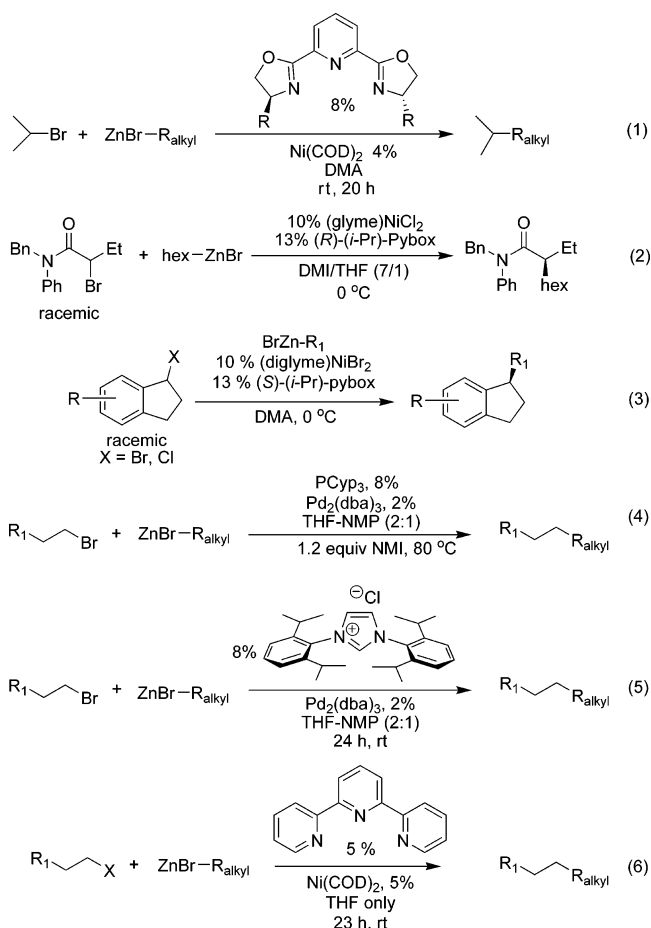
[†] University of Arkansas.

[‡] University of Alabama.

[§] University of Central Arkansas.

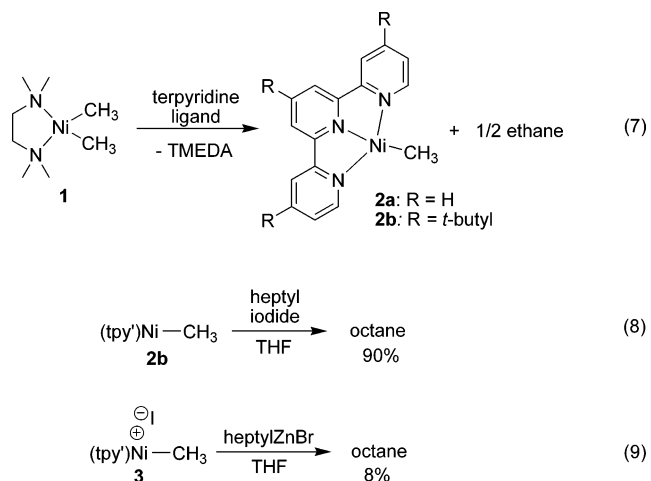
be fully converted to *enantiopure* products with no evidence of kinetic resolution during the catalysis. Although no mechanistic studies to account for the stereo-convergence were reported, the involvement of radicals in these and other systems has been suggested.^{2,3a,b} Additionally, to this point, the electrophiles used for the asymmetric cross-coupling reaction have all been activated, with success only being reported for the α -bromo amides or the benzylic halides.^{1m,2} Moreover, the nickel/pybox-catalyzed reactions all involve the use of DMA (DMA = *N,N*-dimethylacetamide) or other high boiling additives, thereby potentially limiting their use. Additives, such as NMI (NMI = *N*-methylimidazole), have been reported to enhance the reactivity of alkylzinc reagents,⁴ and the successful use of amides in Negishi cross-couplings has been known for some time.^{1d,e,i-k,5} Fu showed that the yields for alkyl-alkyl cross-couplings with Pd/PCyp₃ (Cyp = cyclopentyl) dropped over 20% when NMP (NMP = *N*-methyl-2-pyrrolidone) was removed from the solvent mixture (eq 4).^{1f} Another striking example of the amide effect was observed by Organ, who noted that substituting THF for NMP in the Pd/*N*-heterocyclic carbene-catalyzed reactions (eq 5) resulted in a drop of overall yield from 75 to 2%.^{1d} We were therefore pleased to report a Ni/terpyridine-catalyzed version of the alkyl-alkyl cross-coupling reaction that permitted the reaction to be run without amide additives in THF solvent (eq 6).^{1a,b} The identification of a ligand system that could catalyze the Negishi couplings in a low boiling, amide-free solvent thus prompted us to look more closely at the organometallic features of the alkyl-alkyl cross-coupling reaction in hopes of obtaining fundamental information that could serve to increase the current scope of the chemistry.

One of the most peculiar features of the terpyridyl ligand system is its ability to stabilize monoalkyl complexes of nickel. Indeed, reaction of (TMEDA)NiMe₂ (**1**) with a terpyridine ligand cleanly led to the formation of (terpyridyl)NiMe (**2**, eq 7). The thermal stability of **2** has then enabled a number of key studies on alkyl transfer reactions to be performed,^{1b} providing initial insights into the mechanism of nickel-mediated alkyl-alkyl cross-coupling reactions. It has been shown that **2** can effectively transfer its methyl group to alkyl iodides, affording cross-coupled alkanes in high yields, as exemplified in eq 8

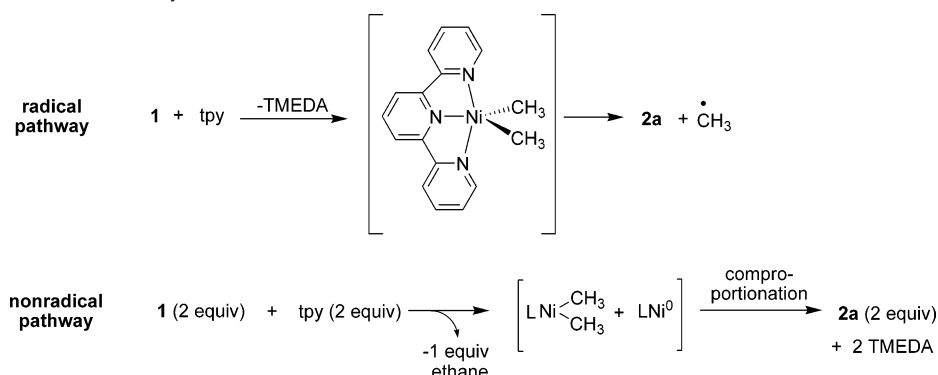


(tpy' = 4,4',4''-tri-*tert*-butylterpyridine).^{1a,b} Surprisingly, however, the closely related Ni(II)-alkyl halide complex **3** did not react with excess transmetalating agent to afford the same product (eq 9).^{1b} This result argues against a two-electron mechanism in a catalytic cycle by which a (terpyridyl)Ni(0) fragment oxidatively adds an alkyl halide to produce **3** and subsequently undergoes a simple transmetalation reaction to afford cross-coupled product.

- (1) (a) Anderson, T. J.; Jones, G. D.; Vivic, D. A. *J. Am. Chem. Soc.* **2004**, *126*, 8100–8101 [erratum p11113]. (b) Jones, G. D.; McFarland, C.; Anderson, T. J.; Vivic, D. A. *Chem. Commun.* **2005**, 4211–4213. (c) Cardenas, D. J. *Angew. Chem., Int. Ed.* **2003**, *42*, 384–387. (d) Hadei, N.; Kantchev, E. A. B.; O'Brien, C. J.; Organ, M. G. *Org. Lett.* **2005**, *7*, 3805–3807. (e) Hadei, N.; Kantchev, E. A. B.; O'Brien, C. J.; Organ, M. G. *J. Org. Chem.* **2005**, *70*, 8503–8507. (f) Zhou, J.; Fu, G. C. *J. Am. Chem. Soc.* **2003**, *125*, 12527–12530. (g) Zhou, J.; Fu, G. C. *J. Am. Chem. Soc.* **2003**, *125*, 14726–14727. (h) Terao, J.; Todo, H.; Watanabe, H.; Ikumi, A.; Kambe, N. *Angew. Chem., Int. Ed.* **2004**, *43*, 6180–6182. (i) Giovannini, R.; Stuedemann, T.; Devasagayaraj, A.; Dussin, G.; Knochel, P. *J. Org. Chem.* **1999**, *64*, 3544–3553. (j) Giovannini, R.; Stuedemann, T.; Dussin, G.; Knochel, P. *Angew. Chem., Int. Ed.* **1998**, *37*, 2387–2390. (k) Jensen, A. E.; Knochel, P. *J. Org. Chem.* **2002**, *67*, 79–85. (l) Netherton, M. R.; Fu, G. C. *Adv. Synth. Catal.* **2004**, *346*, 1525–1532. (m) Fischer, C.; Fu, G. C. *J. Am. Chem. Soc.* **2005**, *127*, 4594–4595. (n) Netherton, M. R.; Fu, G. C. *Top. Organomet. Chem.* **2005**, *14*, 85–108. (o) Netherton, M. R.; Dai, C.; Neuschuetz, K.; Fu, G. C. *J. Am. Chem. Soc.* **2001**, *123*, 10099–10100. (p) Terao, J.; Watanabe, H.; Ikumi, A.; Kuniyasu, H.; Kambe, N. *J. Am. Chem. Soc.* **2002**, *124*, 4222–4223. (q) Hills, I. D.; Netherton, M. R.; Fu, G. C. *Angew. Chem., Int. Ed.* **2003**, *42*, 5749–5752. (r) Frisch, A. C.; Beller, M. *Angew. Chem., Int. Ed.* **2005**, *44*, 674–688. (2) Arp, F. O.; Fu, G. C. *J. Am. Chem. Soc.* **2005**, *127*, 10482–10483. (3) (a) Castano, A. M.; Echavarren, A. M. *Organometallics* **1994**, *13*, 2262–2268. (b) Gonzalez-Bobes, F.; Fu, G. C. *J. Am. Chem. Soc.* **2006**, *128*, 5360–5361. (4) Inoue, S.; Yokoo, Y. *J. Organomet. Chem.* **1972**, *39*, 11–16. (5) (a) Piber, M.; Jensen, A. E.; Rottlaender, M.; Knochel, P. *Org. Lett.* **1999**, *1*, 1323–1326. (b) Dai, C.; Fu, G. C. *J. Am. Chem. Soc.* **2001**, *123*, 2719–2724.



The unique structure and stability of **2**, as well as its probable involvement in a catalytic cycle, warranted further studies of this paramagnetic organometallic compound. Magnetic and DFT studies of **2** interested us, in particular, as we reasoned that if

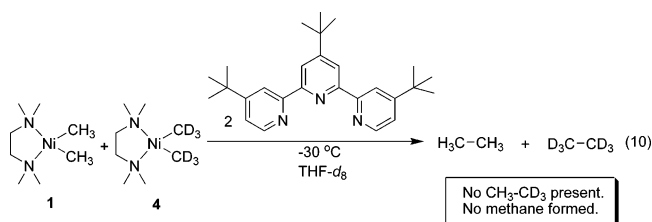
Scheme 2. Possible Reaction Pathways to **2a**

trends between the *electronic* structures of the catalysts with activities can be observed with terpyridine and other ligands then one may be able to rationally optimize future catalysts to ultimately increase the efficiency and scope of the cross-coupling reaction. Here we report new details on the mechanism of the formation of **2**, EPR and unrestricted DFT analyses of **2**, and the trends observed in the catalytic reactivity of a large pool of related ligand derivatives.

Results and Discussion

The formation of **2a** from **1** (eq 7) can be envisioned to proceed by a number of different mechanisms, two of which are outlined in Scheme 2. The first pathway involves displacement of TMEDA by the terpyridine ligand to produce a five-coordinate nickel–dialkyl intermediate, which then undergoes reductive homolysis to produce **2a** and a methyl radical (Scheme 2, top). In this mechanism, ethane can then be formed by the combination of two methyl radicals to produce the half-equivalent of ethane observed in solution. Alternatively, in a “nonradical” pathway, addition of terpyridine can slowly lead to a ligand-induced loss of ethane, in which the resulting Ni(0) fragment then undergoes a comproportionation reaction with a remaining Ni(II)–dimethyl species to afford **2a** (Scheme 2, bottom). For each of the Ni(0) and Ni(II) fragments in the nonradical pathway, L is undefined and may consist of partially bound diamine, terpyridine, or both. To ascertain whether such radical or nonradical pathways were involved in the formation of **2**, addition of tpy’ to a mixture of **1** and (TMEDA)Ni(CD₃)₂ (**4**) in THF-*d*₈ was performed, and the resulting ethane that was formed was analyzed by ¹H and ²H NMR spectroscopy (tpy’ was used for solubility considerations). If ethane was produced by a combination of two methyl radicals (Scheme 2, top), then a statistical mixture of CH₃–CH₃, CH₃–CD₃, and CD₃–CD₃ would be expected. CH₃–CD₃ can be distinguished by its signature ¹H NMR spectrum.⁶ If, however, the reaction proceeded in a nonradical pathway (Scheme 2, bottom), then only CH₃–CH₃ and CD₃–CD₃ would be expected, as the ethane would result from a reductive elimination reaction. The experimental observation is that only CH₃–CH₃ and CD₃–CD₃ was observed (eq 10). Methane might also be expected to form from a hydrogen atom abstraction from THF solvent, but no methane nor any of its isotopomers were observed by NMR spectroscopy. The data thus support a mechanism by which ethane is produced via a nonradical pathway, triggered by the addition of a

terpyridine ligand. Indeed, Porschke and co-workers noted that, upon addition of π -acceptors to **1**, ethane can be formed at temperatures as low as -78 °C.⁷



Notably, the overall reaction described in eq 7 also proceeds with a net reduction of the organometallic species. A reduction to an odd-electron species can be confirmed by EPR spectroscopy, and complex **2a** provides a strong unresolved EPR signal with isotropic $g = 2.021 \pm 0.002$ at room temperature in THF solution (Figure 1a). The same solution when frozen at 77 K exhibits a rhombic signal with $g_1 = 2.056$, $g_2 = 2.021$, and $g_3 = 1.999$ (Figure 1b). The $g_{\text{iso}} = (g_1 + g_2 + g_3)/3$ determined from the rhombic g tensor is similar to the fluid solution g value. This confirms that the same species was detected in solution and at 77 K. Interestingly, the g values suggest a more organic-based radical rather than a metal-centered one, implying that the charge-transfer state consisting of a Ni(II)–methyl cation and a reduced ligand (Chart 1) is the ground-state structure; g values for radicals in extended organic π -systems typically fall in the range of 2.003–2.005,⁸ whereas a four-coordinate Ni(I) complex was previously reported to have a g value close to 2.18.⁹ Budzelaar and co-workers had observed a similar ligand reduction phenomenon with cobalt complexes of the tridentate diiminopyridine ligands.¹⁰ Additionally, nickel complexes of diiminobenzosemiquinonate have been shown to exist in the ground state with an unpaired electron residing on the reduced ligand,¹¹ and reduction of bound terpyridine ligands has also been observed to occur upon addition of terpyridine to ytterbocene complexes.¹² Perhaps most relevant to this work is Gray

(6) Slaughter, L. M.; Wolczanski, P. T.; Klinckman, T. R.; Cundari, T. R. *J. Am. Chem. Soc.* **2000**, *122*, 7953–7975.

(7) Kaschube, W.; Porschke, K. R.; Wilke, G. *J. Organomet. Chem.* **1988**, *355*, 525–532.
 (8) Leffler, J. E. *An Introduction to Free Radicals*; Wiley-Interscience: New York, 1993.
 (9) Ge, P.; Riordan, C. G.; Yap, G. P. A.; Rheingold, A. L. *Inorg. Chem.* **1996**, *35*, 5408–5409.
 (10) Knijnenburg, Q.; Hettterscheid, D.; Kooistra, T. M.; Budzelaar, P. H. M. *Eur. J. Inorg. Chem.* **2004**, 1204–1211.
 (11) Herebian, D.; Bothe, E.; Neese, F.; Weyhermueller, T.; Wieghardt, K. *J. Am. Chem. Soc.* **2003**, *125*, 9116–9128.
 (12) Kuehl, C. J.; Da Re, R. E.; Scott, B. L.; Morris, D. E.; John, K. D. *Chem. Commun.* **2003**, 2336–2337.

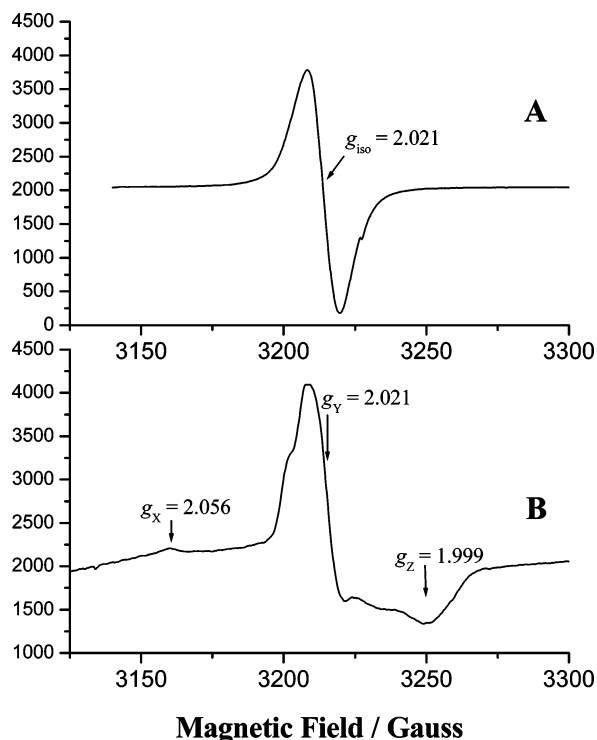
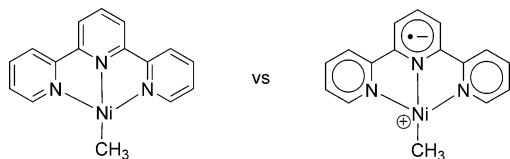


Figure 1. X-band EPR spectra of **2a** in THF (a) in fluid solution at room temperature, (b) in frozen glass at 77 K. Parameters: microwave frequency 9.095 GHz; microwave power 5 mW; modulation amplitude 1 G; gain 2×10^3 .

Chart 1. Representations of **2a** as a Ni(I)–Methyl Complex (left) and the Charge-Transfer State Comprising a Ni(II)–Alkyl Cation (right)



and co-workers' report of ligand reduction in the closely related (terpyridine)PtCl complex.¹³

The g tensors of frozen solution EPR spectra are sensitive to even small contribution from a metal to the singly occupied molecular orbital (SOMO), with the deviation $\Delta g = g - g(\text{electron})$ depending on the spin–orbit coupling. The obtained rhombic spectrum displays $g_1 > g_2 \sim 2.0 \gg g_3$ and $g_3 < 2.0$, suggesting a minor contribution of the metal d -orbital in the SOMO.¹⁴ Assuming similar electronic factors and a similar coordinate system as Gray's description of (tpy)PtCl,¹³ estimates of expected g values for nickel can be made based on the difference between the first ionization energy (IE) of platinum and nickel and their respective M^{+1} spin–orbit coupling values.¹⁵ Using the difference in the first IE as a rough estimate of the difference in energy of the $5d$ -orbitals on platinum versus the $3d$ -orbitals on nickel, then the nickel d -orbitals are roughly $10\,000\text{ cm}^{-1}$ closer in energy than those of platinum to the terpyridyl π^* -orbital. This in turn increases the probability of

overlap of nickel electron density with the LUMO of the terpyridine ligand (the SOMO in the ligand radical anion). These ideas are summarized in Figure 2.

From Gray et al.,¹³ $g_y = (g_e + 2\xi\rho_d/\Delta E)$, where g_e = free electron value = 2.0023, ξ = one-electron spin–orbit coupling for M^+ (Ni: 565 cm^{-1} , Pt: 3400 cm^{-1}),¹⁴ and ρ_d is the nickel $3d_{yz}$ contribution to the SOMO. Moreover

$$g_y - g_e = 2.021 - 2.0023 = 0.0187 = 2\xi\rho_d/\Delta E = 2(565\text{ cm}^{-1})\rho_d/\Delta E \text{ (ref 13)}$$

Then, assuming $\Delta E = \sim 15\,000\text{ cm}^{-1}$ (Figure 2), this gives $\rho_d = 0.25$. This value for ρ_d seems reasonable, as Figure 3 shows a small, but clear, contribution of the nickel d_{yz} to the SOMO. The value is also not so low (<0.1) that there is negligible nickel contribution, but then not so high (>0.5) that the orbital is more metal than ligand character. The UV data (Table 1) of **2** are also consistent with the reduced character of the ligand, as the spectra are strikingly similar to those of Na(tpy)₂.

The unusual electronic structure of **2** suggested by the EPR data can have large implications for cross-coupling catalysis, as activities may correlate with the ability of the tridentate ligands to stabilize a radical anion. To further expound this intriguing EPR result, DFT calculations (unrestricted B3LYP/m6-31G*; see Experimental Section) were performed on **2a** in order to determine the spatial distribution of the spin density. Geometry optimization yielded a planar (except for the methyl hydrogens), approximately square complex, the geometry of which agrees well with the X-ray crystal structure.^{1a} The calculated and measured bond lengths are compared in Table 2.¹⁶ A number of population analyses were also included in the DFT calculations, and all show that the majority of the spin density in **2a** resides on the terpyridine ligand (Table 3). An isodensity representation of the SOMO of **2a**, depicted in Figure 3, also shows that the unpaired electron is delocalized over the aromatic ligand. The spin density calculations in the planar conformation are thus in full agreement with the EPR data and support a ground-state structure that is most properly described as a nickel(II)–alkyl cation bearing a reduced terpyridine ligand. Interestingly, the SOMO shows antibonding interactions between the central nitrogen with nickel, suggesting that, upon oxidation, this bond should shorten.¹⁷ However, this is not observed experimentally (Table 2), likely due to the short Ni–Ni contacts observed in the crystal structure of **3**.^{1b} The calculations also show a large amount of radical character at the carbons ortho and para to the central nitrogen of the terpyridine ring. Kiplinger has reported alkyl migration to these sites in terpyridine lutetium complexes.¹⁸ Although we have never observed analogous chemistry with the nickel complexes, we cannot rule out such species in a catalytic cycle at this time.

We have also determined optimized geometries and energies of **2a**, constraining the N_2 –Ni–C bond angle to five values between 180 and 120° , to explore the effect of the catalyst geometry on the electronic structure. Figure 4 shows that the N_2 –Ni–C angle can bend about 15° without raising the energy more than 1 kcal/mol. However, substantial bends require

(13) Hill, M. G.; Bailey, J. A.; Miskowski, V. M.; Gray, H. B. *Inorg. Chem.* **1996**, *35*, 4585–4590.

(14) Goodman, B. A.; Raynor, J. B. *Adv. Inorg. Chem. Radiochem.* **1970**, *13*, 135–362.

(15) Huheey, J. E. *Inorganic Chemistry, Principles of Structure and Reactivity*, 3rd ed.; Harper and Row: New York, 1983; pp 42–44.

(16) Because of the large errors in the X-ray structure of **2a**, a comparison to the experimentally derived bond lengths is not appropriate.

(17) We thank a reviewer for pointing this out.

(18) Jantunen, K. C.; Scott, B. L.; Hay, P. J.; Gordon, J. C.; Kiplinger, J. L. *J. Am. Chem. Soc.* **2006**, *128*, 6322–6323.

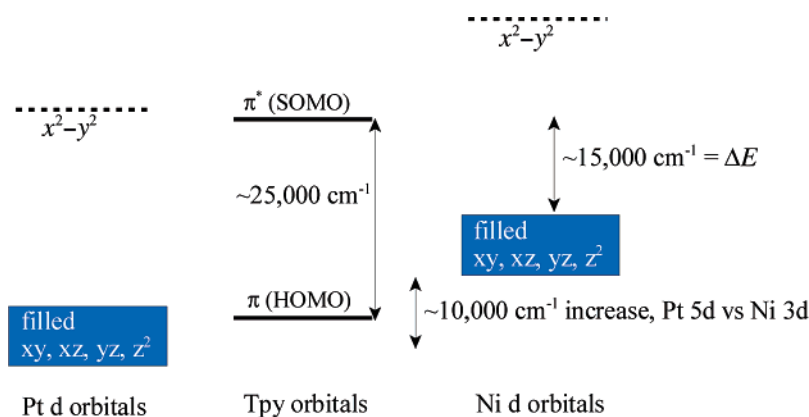


Figure 2. Molecular orbital diagram for platinum and nickel complexes of terpyridine, based on ref 13.

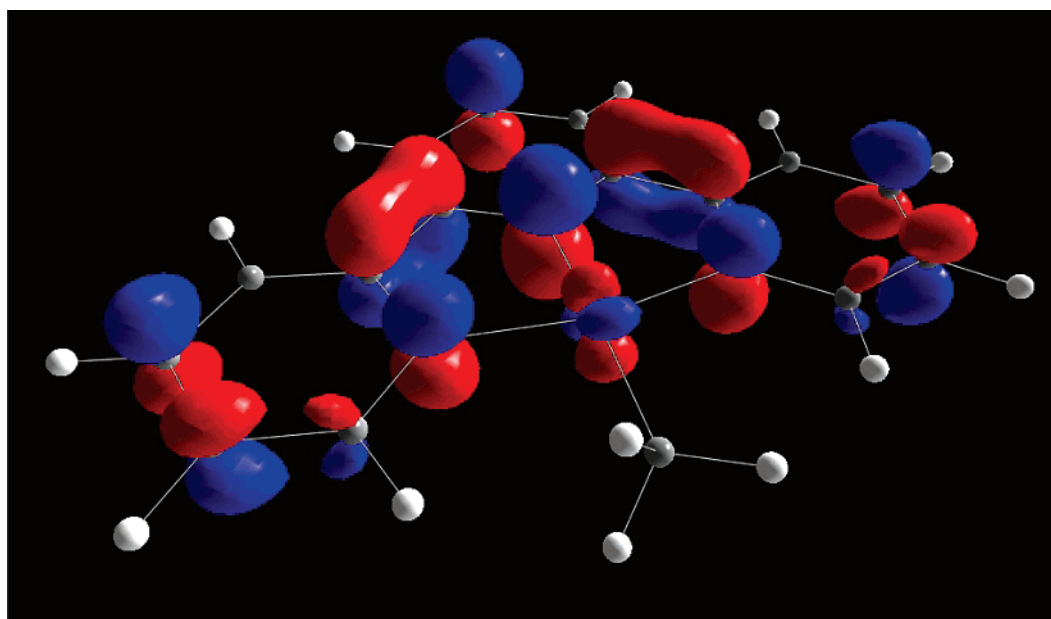


Figure 3. Singly occupied molecular orbital of complex **2a** from unrestricted DFT calculations.

Table 1. UV–Visible Data of Reduced Terpyridyl Compounds

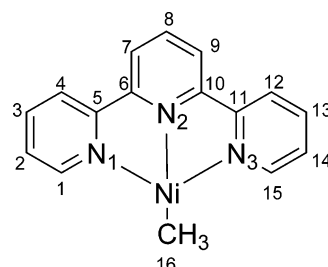
compound	λ_{max} (nm)	solvent	ϵ (L mol ⁻¹ cm ⁻¹) $\times 10^3$
2a	220, 270, 384,	THF	10.1, 12.1, 5.63, 1.55,
	538, 576		1.86
2b	220, 270, 380,	THF	26.6, 25.0, 11.4, 3.41,
	544, 584		3.97
Na(tpy) ₂	216, 242, 280,	THF	15.7, 22.6, 21.7, 1.51,
	380, 450, 606		1.13, 3.44

10–15 kcal/mol. DFT calculations at these strongly bent geometries predict that the spin density on the nickel increases relative to the planar form (see Table 3 for a representative example). This additional insight provided by the DFT studies suggests that ligands that effect the positioning of the pendant alkyl group relative to the plane of the other three nitrogen atoms can thus, in theory, modulate this charge-transfer chemistry by allowing or not allowing optimum overlap of the d_{yz} -orbital with the nitrogen of the central pyridyl ring of the ligand as represented in the SOMO (Figure 3).

To complement the EPR and DFT studies, comparative cross-coupling reactions were performed with the ligands shown in Chart 2. We chose iodo- and bromopropylbenzene as our alkyl electrophiles and *n*-pentylzinc bromide as our alkyl nucleophile (Table 4). Table 4 lists all of the cross-coupling yields obtained

for the ligand survey. While solubility effects dominate the difference in yields observed with ligands **5** and **6**,^{1b} we find here that, upon making the terpyridine ligand more electron rich as in **7** and **8**, a substantial decrease in yields for the cross-coupling reaction results. However, decreases in yields were also observed when electron-poor terpyridine ligands, such as **9–11**, were used. Steric effects with the terpyridine-based ligands were quite dramatic, as it was found that placing methyl groups in the 6 and 6'' positions of the terpyridine ligand (**12**) shuts down the catalysis almost entirely. The π -extended ligands **13** and **14** showed quite respectable yields, but did not outperform tpy'. The slightly better performance of **13** over **14**, especially in the cross-coupling of alkyl bromides, is not well-understood at this point and is currently the subject of further investigation. Connick and co-workers noted that platinum complexes of **15** and **16** had more negative oxidation potentials than the analogous terpyridine complex,²¹ so we were curious how the cross-coupling catalysis would proceed with these

- (19) Bessel, C. A.; See, R. F.; Jameson, D. L.; Churchill, M. R.; Takeuchi, K. *J. J. Chem. Soc., Dalton Trans.* **1992**, 3223–3228.
 (20) Glendening, E. D.; Badenhop, J. K.; Reed, A. E.; Carpenter, J. E.; Bohmann, J. A.; Morales, C. M.; Weinhold, F. *NBO 5.0*; University of Wisconsin, Madison: Theoretical Chemistry Institute, 2001.
 (21) Willison, S. A.; Jude, H.; Antonelli, R. M.; Rennekamp, J. M.; Eckert, N. A.; Bauer, J. A. K.; Connick, W. B. *Inorg. Chem.* **2004**, *43*, 2548–2555.

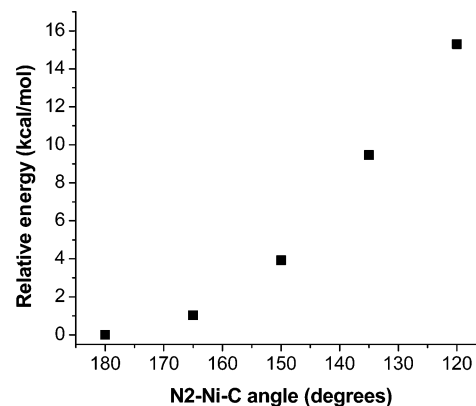
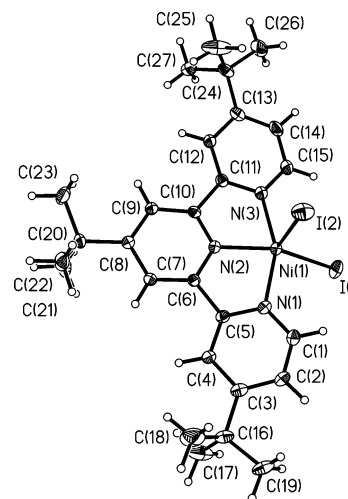
Table 2. Calculated Bond Lengths (Å) and Angles (°) Found in **2a** versus Those Found Experimentally in Related Derivatives


bond or angle	2a (calcd)	free terpyridine ¹⁹	2b (X-ray)	3 (X-ray)
Ni–C ₁₆	1.935		1.944(4)	1.921(9)
Ni–N ₁	1.929		1.903(3)	1.927(9)
Ni–N ₂	1.867		1.845(3)	1.880(7)
Ni–N ₃	1.929		1.914(3)	1.923(8)
N ₁ –C ₁	1.351	1.339(9)	1.356(4)	1.336(11)
N ₁ –C ₅	1.389	1.317(7)	1.385(4)	1.370(11)
N ₂ –C ₆	1.364	1.353(8)	1.358(4)	1.349(10)
N ₂ –C ₁₀	1.364	1.349(7)	1.355(4)	1.328(11)
N ₃ –C ₁₁	1.389	1.350(8)	1.377(4)	1.384(10)
N ₃ –C ₁₅	1.351	1.344(9)	1.350(4)	1.346(11)
C ₁ –C ₂	1.384	1.391(10)	1.364(5)	1.370(13)
C ₂ –C ₃	1.407	1.351(10)	1.403(5)	1.385(13)
C ₃ –C ₄	1.384	1.388(9)	1.384(4)	1.416(12)
C ₄ –C ₅	1.402	1.349(8)	1.403(4)	1.364(13)
C ₅ –C ₆	1.449	1.488(8)	1.450(4)	1.489(11)
C ₆ –C ₇	1.392	1.398(9)	1.390(4)	1.371(11)
C ₇ –C ₈	1.403	1.376(9)	1.393(4)	1.402(12)
C ₈ –C ₉	1.403	1.380(9)	1.413(4)	1.401(12)
C ₉ –C ₁₀	1.392	1.396(8)	1.378(4)	1.387(12)
C ₁₀ –C ₁₁	1.449	1.493(8)	1.455(4)	1.465(12)
C ₁₁ –C ₁₂	1.402	1.391(9)	1.396(4)	1.370(13)
C ₁₂ –C ₁₃	1.384	1.386(9)	1.384(4)	1.405(12)
C ₁₃ –C ₁₄	1.407	1.366(10)	1.399(5)	1.410(12)
C ₁₄ –C ₁₅	1.384	1.360(10)	1.375(5)	1.379(13)
N ₂ –Ni–Me	174.7		177.19 (12)	175.8 (4)
N ₁ –Ni–N ₂	82.1		81.58 (12)	82.1 (3)

Table 3. Calculated Free Valencies for the Heteroatoms of Terpyridyl Nickel Complexes

population analysis	Compound 2a			(tpy)NiMe with a N ₂ –Ni–C Angle of 144.1°		
	Ni	N ₂	N ₁	Ni	N ₂	N ₁
Lowdin free valencies	0.087	0.179	0.059	0.337	0.187	0.062
Mulliken free valencies	0.076	0.187	0.063	0.331	0.194	0.064
Natural Spin Densities from NBO analysis ²⁰	0.037	0.245	0.090	0.182	0.273	0.082

ligands. While the parent ligand **15** gave yields higher than those seen with terpyridine, we were disappointed that the tetramethylated ligand **16** showed much lower activity for cross-coupling catalysis. Again, the steric environment afforded by the ligand appears to play a major role in catalytic activity, as it was seen that yields with the bispyrazole system once again rose when the methyl groups were positioned away from the metal center as in **17**. Given that the sterics in ligands **12** and **16** discourage a flat geometry, it is tempting to infer that any ligand preventing the flattening of the N₃Ni–R coordination sphere also retards reactivity. Additionally, other ligands deviating in structure from the planar, aromatic triimines, such as **18**–**22**, all showed poor activity. Finally, we see that a tridentate ligand framework is not necessary to achieve catalysis, as the yields obtained with electron-poor bathophenanthroline (**23**) are competitive with those obtained with **14**. It appears, however,

**Figure 4.** Optimized relative energies of (tpy)NiMe as a function of the constrained N₂–Ni–C(Me) angle.**Figure 5.** ORTEP diagram of (tpy')Ni₂. Ellipsoids shown at the 50% level. Selected bond distances (Å): I1–Ni1 2.6027(5), I2–Ni1 2.6248(5), Ni1–N₂ 1.979(2), Ni1–N₁ 2.069(2), Ni1–N₃ 2.092(2). Selected bond angles (°): N₂–Ni1–N₁ 78.52(9), N₂–Ni1–N₃ 78.27(9), N₁–Ni1–N₃ 156.32(9), N₂–Ni1–I1 146.59(6), N₁–Ni1–I1 98.48(6), N₃–Ni1–I1 98.25(6); N₂–Ni1–I2 100.83(6), N₁–Ni1–I2 94.97(6), N₃–Ni1–I2 93.95(6), I1–Ni1–I2 112.576(14).

that an imine-based moiety is required for catalysis, as ligand **24** (which can potentially form an amido complex) is unproductive. Dppz (**25**)²² and dppn (**26**)²³ afforded yields lower than bathophenanthroline.

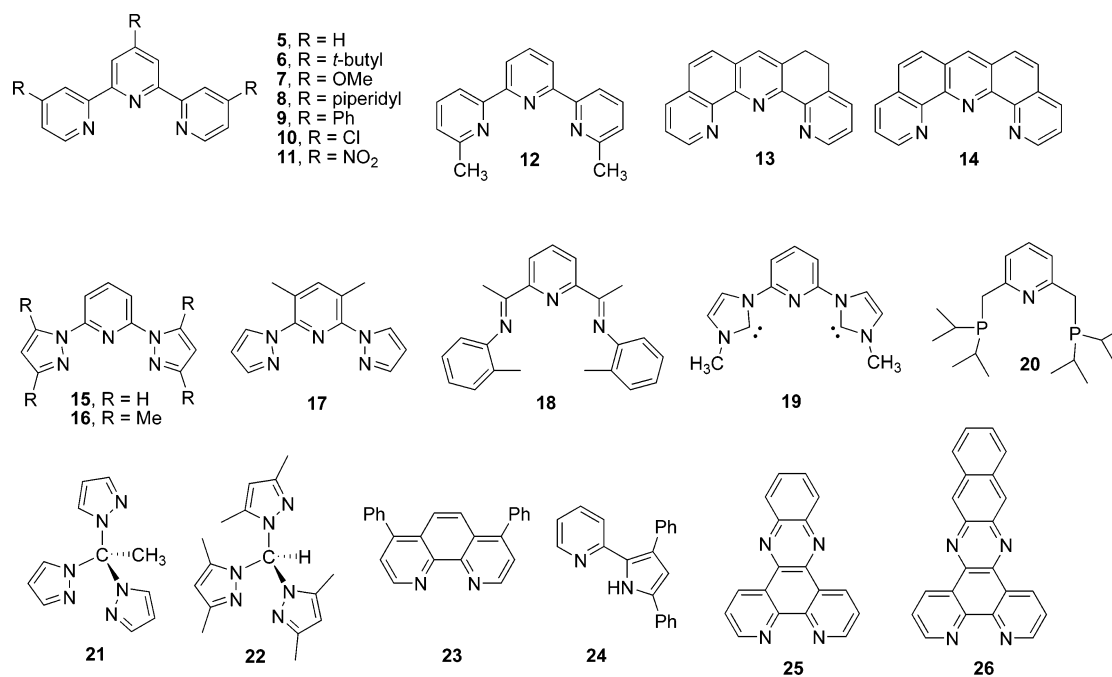
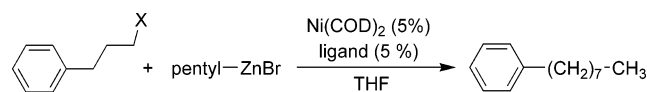
The ligand survey also afforded an opportunity to study the role of the initial nickel source in the cross-coupling reactions. We found that similar yields were obtained whether a ligand was added in situ to commercially available Ni(COD)₂ or whether preformed LNi₂ was used as the starting material (Table 4, entries 2, 20, and 21). One advantage of preparing preformed nickel dihalide complexes is that they are air-stable and can be handled and stored outside of a glovebox.²⁴ Their use also ensures complete ligation of the imines to nickel and rules out any influence of cyclooctadiene in the interpretation of results.²⁵ An X-ray structure of (tpy')Ni₂ was obtained to further support the nature of the nickel diiodides, and the

(22) Greguric, A.; Greguric, I. D.; Hambley, T. W.; Aldrich-Wright, J. R.; Collins, J. G. *J. Chem. Soc., Dalton Trans.* **2002**, 849–855.

(23) Yam, V. W.-W.; Lo, K. K.-W.; Cheung, K.-K.; Kong, R. Y.-C. *J. Chem. Soc., Chem. Commun.* **1995**, 1191–1193.

(24) We found, however, that DMF solutions of (terpyridyl)Ni₂ slowly decomposed to [(terpyridyl)₂Ni]₂. Methylene chloride solutions of (terpyridyl)Ni₂ were stable over much longer times (days).

Chart 2. Ligands Used for Catalytic Studies

Table 4. Effect of Ligand on Yields of Alkyl–Alkyl Cross-Couplings^a

entry	ligand	% yield for X = I	% yield for X = Br
1	5	60	17
2	5 ^b	54	16
3	6	98	46
4	7	53	44
5	8	38	3
6	9	54	33
7	10	19	3
8	10 ^c	44	33
9	11	0	0
10	11 ^c	31	17
11	12	6	4
12	13	63	59
13	14	58	37
14	15	67	45
15	16	13	16
16	17 ^b	63	31
17	18	8	0
18	19	4	1
19	20	1	0
20	21	3 (2 ^b)	0
21	22	5 (8 ^b)	1
22	23	56	43
23	24	3	0
24	25	40	27
25	26	37	23

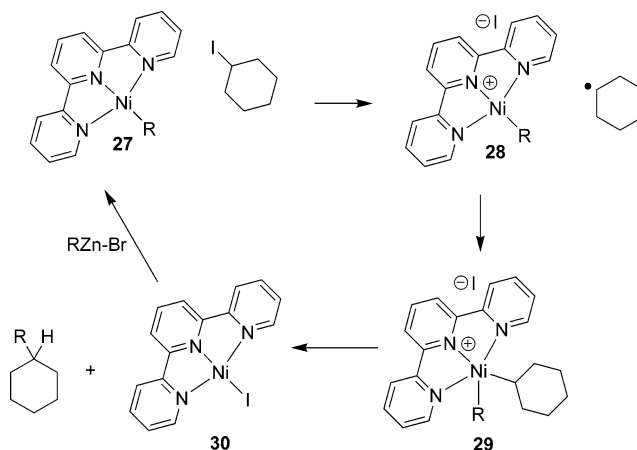
^a Yields calculated by GC relative to an internal standard. ^b Catalyst used was LNiI₂. ^c Catalyst used was LNiCl₂.

ORTEP diagram is shown in Figure 5. This terpyridine-based molecule was found to crystallize in the monomeric, five-coordinate form, similar to (tpy')NiCl₂.²⁶ The use of preformed

(25) In a control experiment, use of Ni(COD)₂ with no added ligand gave no apparent formation of cross-coupled products for both the alkyl bromides and alkyl iodides.

(26) Suzuki, H.; Matsumura, S.; Satoh, Y.; Sogoh, K.; Yasuda, H. *React. Funct. Polym.* **2004**, *59*, 253–266.

Scheme 3. Possible Mechanism for Nickel-Catalyzed Alkyl–Alkyl Negishi Reactions



LNiX₂ complexes did make a difference, however, in the reactivity of ligands that were easy to reduce with nickel(0) (Table 4, entries 7 vs 8 and 9 vs 10). We found that these electron-poor ligands can be attached to an air-stable source of nickel(II) (commercially available (DME)NiCl₂ (DME = 1,2-dimethoxyethane)) without concomitant ligand reduction.

Implications

On the basis of the above studies and previous work,^{1a,b} an updated mechanism for the nickel-catalyzed alkyl–alkyl Negishi reactions is proposed in Scheme 3. This mechanism involves reaction of a (terpyridyl)Ni(alkyl) complex, such as **27**, with an alkyl halide to form **28** and an alkyl radical. The redox potentials of **2a** and **2b** were found to be -1.32 and -1.44 V (vs Ag/Ag⁺ in THF solution),^{1b} making the alkyl halide reduction by **2** thermodynamically favorable. *What has emerged as a new, key feature of this current study is that the alkyl halide reduction by (terpyridine)NiR_{alkyl} is substantially ligand based!* This one-electron, ligand-based redox event is fundamentally a

Table 5. Calculated Free Valencies for Potential Intermediates in a Catalytic Cycle

population analysis	LNiMe L = ligand 23			Compound 29			Compound 30		
	Ni	N2	N1	Ni	N2	N1	Ni	N2	N1
Lowdin free valencies	1.145	0.059	0.059	0.833	0.090	0.023	1.022	0.076	0.039
Mulliken free valencies	1.148	0.061	0.061	0.847	0.090	0.024	1.034	0.076	0.036
natural spin densities from NBO Analysis	1.244	0.003	0.003	0.938	0.143	0.019	1.131	0.015	0.008

new concept in cross-coupling chemistry and may provide some insight into how stereo-convergence might be possible for the asymmetric versions of this reaction using chiral ligands. We speculate that alkyl halide reduction by the ligand leaves an alkyl radical in close proximity to the metal center, where an oxidative radical addition ensues to afford the nickel(III)–dialkyl species **29**. If L is therefore chiral, enantioselective addition of the radical to nickel may take place. Fast reductive elimination of cross-coupled alkane then occurs to release electrons from the antibonding orbital of **29** leaving **30** as the final nickel-containing product of a catalytic cycle. We have already shown that indeed (tpy)NiI is a viable catalyst for alkyl–alkyl Negishi reactions.^{1b} Detailed kinetic studies will be necessary to further support this mechanism, and such studies are being initiated in our labs. Elements of Scheme 3 may also fit a chain-like mechanism, similar to what had been proposed by Kochi.²⁷ With regard to the electronic structures of the proposed intermediates, we can say that spin-unrestricted DFT analyses of **29** and **30** predict that these compounds should be formulated as Ni(III) and Ni(I) complexes, respectively (Table 5). The oxidation states may also be dictated by the nature of the diimine ligand, as we found that bidentate ligands, such as bathophenanthroline, have much different electronic characteristics than the terpyridyl-based counterparts (Table 5).

Experimental Section

General Considerations. All manipulations were performed using standard Schlenk techniques or in a nitrogen-filled drybox, unless otherwise noted. Solvents were distilled from appropriate drying reagents, such as Na/benzophenone or CaH₂. All reagents were used as received from commercial vendors. Pentylzinc bromide was purchased from Rieke Metals, Inc. and used without further purification. Elemental analyses were performed by Desert Analytics. ¹H NMR spectra were recorded at ambient temperature (unless otherwise noted) on a Bruker Avance 300 MHz (75 MHz for ¹³C nuclei) spectrometer and referenced to residual proton or carbon solvent peaks. A Rigaku MSC Mercury/AFC8 diffractometer was used for X-ray structural determinations. Ligands **7**,²⁸ **9**,²⁹ **10**,³⁰ **11**,²⁸ **12**,³¹ **13**,³² **14**,³² **15**,²¹ **16**,³³ **19**,³⁶ **20**,³⁴ **21**,³³ **22**,³⁵ and **24**³⁷ were synthesized according to previously

published procedures. Complexes **2a** and **2b**^{1a,b} were synthesized according to previously published procedures. The alkyl–alkyl cross-coupling reactions in Table 4 were performed by previously published procedures.^{1b}

UV–Visible Measurements. Solutions of **2a**, **2b**, and Na(tpy)₂ in THF were prepared in a nitrogen glovebox and placed in quartz cuvettes (1 cm path length) capped with a Teflon stopper and wrapped tightly with Parafilm. The UV–visible spectra were collected using a HP 8452A diode array spectrophotometer using a spectral window of 190–820 nm wavelengths.

Electronic Structure Calculations. Quantum calculations were performed with the PQS 3.2 software.³⁸ Initial geometries were constructed using PCModel 8.5³⁹ and preoptimized via the MMX force field. Both constrained and unconstrained geometry optimizations were performed using the B3LYP exchange–correlation functional⁴⁰ and the m6-31G* basis set.⁴¹ Note that the most consistent definition of the SOMO of a doublet state is the charge natural orbital whose occupation number is close to 1, and this was used in this work. The occupation number in the case of **2a** was exactly 1.

EPR Measurements. Solutions of **2a** in THF (10^{−2}–10^{−3} M) were prepared under nitrogen in a drybox, placed in quartz EPR tube (o.d. = 4 mm, WILMAD), degassed before use by three freeze–pump–thaw cycles, and the tube was sealed. EPR spectra were measured at X-band (9 GHz) using a Bruker ESP 300 spectrometer equipped with a Bruker ER035M gaussmeter and a HP 5352B microwave frequency counter for g value determination.

Synthesis of Na(tpy)₂. In a nitrogen-filled glovebox, sodium metal (32 mg, 1.41 mmol), which had been pressed, was stirred in 6 mL of THF. A separate solution of tpy (655 mg, 2.81 mmol) in 14 mL of THF was then added slowly via pipet. Within 10 min, the yellow solution became dark green in color. After 1 h of stirring, the THF was removed via high vacuum manifold. The solid was collected and dried for an additional 2 h, yielding 492 mg (71%) of material. The solid was used without further purification.

Synthesis of (TMEDA)Ni(CD₃)₂ (4**):** (TMEDA)Mg(CD₃)₂ was prepared analogously to (TMEDA)Mg(CH₃)₂⁴² with the substitution of CD₃I for CH₃I. Compound **4** was then synthesized in 61% yield from (TMEDA)Mg(CD₃)₂ and (TMEDA)Ni(acac)₂ as previously reported for the synthesis of (TMEDA)Ni(CH₃)₂.⁴³ ¹H NMR (THF-*d*₈, −40 °C): δ 2.28 (s, 12H), 2.13 (s, 4H). ²H NMR (THF-*d*₈, −40 °C): δ −1.43 (s). ¹³C NMR (THF-*d*₈, −40 °C): δ 59.3 (s), 46.6 (s), −12.7 (septet, ¹J_{C–D} = 18.5 Hz).

Isotopic Labeling Study for Scheme 2: To a vial cooled to −30 °C were added (TMEDA)Ni(CH₃)₂ (11 mg, 0.054 mmol) and (TMEDA)Ni(CD₃)₂ (11 mg, 0.054 mmol) in THF-*d*₈ (0.5 mL). This solution was added to a precooled J. Young type NMR tube. To the NMR tube was added a solution of tpy' (43 mg, 0.11 mmol) in THF-*d*₈ (0.5 mL), and the Teflon cap to the NMR tube was immediately closed. The NMR tube was shaken vigorously and allowed to warm to room temperature.

- (27) (a) Tsou, T. T.; Kochi, J. K. *J. Am. Chem. Soc.* **1979**, *101*, 7547–7560.
 (b) Tsou, T. T.; Kochi, J. K. *J. Am. Chem. Soc.* **1979**, *101*, 6319–6332.
 (c) Morrell, D. G.; Kochi, J. K. *J. Am. Chem. Soc.* **1975**, *97*, 7262–7270.
 (28) Case, F. H. *J. Org. Chem.* **1962**, *27*, 640–641.
 (29) Case, F. H.; Kasper, T. J. *J. Am. Chem. Soc.* **1956**, *78*, 5842–5844.
 (30) Hobert, S. E.; Carney, J. T.; Cummings, S. D. *Inorg. Chim. Acta* **2001**, *318*, 89–96.
 (31) Sato, Y.; Nakayama, Y.; Yasuda, H. *J. Organomet. Chem.* **2004**, *689*, 744–750.
 (32) Hung, C.-Y.; Wang, T.-L.; Jang, Y.; Kim, W. Y.; Schmehl, R. H.; Thummel, R. P. *Inorg. Chem.* **1996**, *35*, 5953–5956.
 (33) Reger, D. L.; Grattan, T. C. *Synthesis* **2003**, 350–356.
 (34) Jameson, D. L.; Goldsby, K. A. *J. Org. Chem.* **1990**, *55*, 4992–4994.
 (35) Reger, D. L.; Grattan, T. C.; Brown, K. J.; Little, C. A.; Lamba, J. J. S.; Rheingold, A. L.; Sommer, R. D. *J. Organomet. Chem.* **2000**, *607*, 120–128.
 (36) Peris, E.; Mata, J.; Loch, J. A.; Crabtree, R. H. *Chem. Commun.* **2001**, 201–202.
 (37) Klappa, J. J.; Rich, A. E.; McNeill, K. *Org. Lett.* **2002**, *4*, 435–437.

- (38) PQS, version 3.2; Parallel Quantum Solutions, 2013 Green Acres Road, Fayetteville, AR 72703.
 (39) PCMODEL for Windows 8.50.0, September 2003, Serena Software.
 (40) Becke, A. D. *J. Chem. Phys.* **1993**, *98*, 5648–5652.
 (41) Mitin, A. V.; Baker, J.; Pulay, P. *J. Chem. Phys.* **2003**, *118*, 7775–7782.
 (42) Anderson, R. A.; Wilkinson, G. *Inorg. Synth.* **1979**, *19*, 262–265.
 (43) Yamamoto, T.; Yamamoto, A.; Ikeda, S. *J. Am. Chem. Soc.* **1971**, *93*, 3350–3359.

After standing for 2 days and being shaken periodically to allow for adequate mixing, the ^1H NMR spectrum was obtained. No formation of CD_3CH_3 was detected, only CH_3CH_3 . Using the free TMEDA ligand as the internal standard, the yield of CH_3CH_3 was 0.0468 mmol, 43%. It is noted that a control sample of CD_3CH_3 was easily detected at 0.025 mmol. ^1H NMR of CH_3CH_3 (300.13 MHz, $\text{THF-}d_8$, 233 K): δ 0.86 (s). ^1H NMR of CD_3CH_3 (300.13 MHz, $\text{THF-}d_8$, 296 K): δ 0.82 (septet, $J_{\text{H-C-C-D}} = 1.2$ Hz). ^2H NMR (proton decoupled) of CD_3CH_3 (46.07 MHz, $\text{THF-}d_8$, 296 K): δ 0.81 (s). ^{13}C NMR (75.47 MHz, $\text{THF-}d_8$, 296 K): δ 6.85 (septet, $J_{\text{C-D}} = 0.6$ Hz).

Synthesis of Ligand 8: 4,4',4''-Trichloro-2,2':6',2''-terpyridine³⁰ (490 mg, 1.46 mmol) and $\text{MnCl}_2(\text{H}_2\text{O})_4$ (605 mg, 3.1 mmol) were suspended in 50 mL of dry MeOH, and then 15 g of freshly distilled piperidine was added. The mixture was heated to reflux for 20 h. The resulting mixture was cooled, and the solvents were removed via a rotovap. To the residue was then added 5 g of KOH in 100 mL of H_2O and 100 mL of MeCN. This suspension was stirred open to air for 24 h at room temperature. The organics were then extracted with CH_2Cl_2 and dried with MgSO_4 . Yield: 511 mg, 73%. ^1H NMR (CDCl_3 , 22 °C): δ 8.34 (d, $J = 6.0$ Hz, 2H), 8.16 (d, $J = 2.6$ Hz, 2H), 7.87 (s, 2H), 6.69 (dd, $J = 6.0, 2.8$ Hz, 2H), 3.56 (bt, $J = 5.3$ Hz, 4H), 3.48 (bt, $J = 4.7$ Hz, 8H), 1.73–1.66 (bm, 18H). ^{13}C NMR (CDCl_3 , 25 °C): δ 156.9, 156.7, 155.8, 155.3, 148.6, 107.9, 105.8, 105.3, 47.7, 47.4, 25.5, 25.3, 24.5, 24.4. HRMS calcd for $\text{C}_{30}\text{H}_{38}\text{N}_6$: 483.3236. Observed: 483.3236

Synthesis of Ligand 17: Synthesis was analogous to that for 2,6-bis(*N*-pyrazolyl)pyridine reported by Jameson.³⁴ Under N_2 was heated at 75 °C a 20 mL solution of pyrazole (1.198 g, 17.6 mmol) and potassium metal (649 mg, 16.6 mmol) in diglyme until the potassium metal dissolved (1–2 h). 2,6-Dibromo-3,5-dimethylpyridine⁴⁴ (1.466 g, 5.53 mmol) was added at once and the solution heated to 110 °C for 4 days. Workup was completed as reported by Jameson. Yield 1.136 g, 86%. ^1H NMR (CDCl_3 , 300.13 MHz, 23 °C): δ 8.24 (dd, $J = 2.5, 0.7$ Hz, 2H), 7.75 (dd, $J = 1.6, 0.6$ Hz, 2H), 7.64 (t, $J = 0.7$ Hz, 1H), 6.45 (dd, $J = 2.6, 0.7$ Hz, 2H), 2.59 (d, $J = 0.7$ Hz, 6H). ^{13}C NMR (CDCl_3 , 75.47 MHz, 23 °C): δ 147.2, 146.5, 141.3, 129.9, 124.5, 106.8, 19.1. Anal. Calcd (found) for $\text{C}_{13}\text{H}_{13}\text{N}_5$: C, 65.18 (65.25); H, 5.67 (5.48).

(44) Dunn, A. D.; Guillermic, S. Z. *Chem.* **1988**, 28, 59–60.

Synthesis of (tpy)NiI₂ as a Representative Synthesis of LNiI₂ Compounds: To a solution of $\text{Ni}(\text{COD})_2$ (475 mg, 1.73 mmol) in 50 mL of THF was added a solution of tpy (411 mg, 1.76 mmol) in 20 mL of THF. This green solution was stirred for 5 min at which point a solution of I_2 (441 mg, 1.74 mmol) in 20 mL of THF was cannulated resulting in an immediate color change to orange. The reaction was stirred for 1 h followed by filtering of the orange solid using a glass frit. The solid was washed with 40 mL of diethyl ether and dried on the high vacuum manifold for 4 h. Yield 942 mg, 1.73 mmol, quantitative. Anal. Calcd (found) for $\text{C}_{15}\text{H}_{11}\text{I}_2\text{N}_3\text{Ni}$: C, 32.94 (33.01); H, 2.24 (2.03).

Synthesis of (4,4',4''-Trichloroterpyridine)NiCl₂ as a Representative Synthesis of LNiCl₂ Compounds: A mixture of $(\text{DME})\text{NiCl}_2$ (150 mg, 0.684 mmol) and **10** (229 mg, 0.683 mmol) in THF (10 mL) was heated at reflux for 15 h. The resulting light green precipitate was collected on a glass-fritted funnel and washed with THF, Et_2O , and pentane. The light green solid was dried on a high vacuum manifold, yielding 294 mg (92%) of product.

Acknowledgment. D.A.V. thanks the Chemical Sciences, Geosciences and Biosciences Division, Office of Basic Energy Sciences, Office of Science, of the U.S. Department of Energy (DE-FG02-06ER15801), the Arkansas Biosciences Institute, and the NIH (RR-015569-06) for support of this work. P.P. acknowledges support by the National Science Foundation (CHE-0515922). The authors thank Kevin Shaughnessy for help with EPR experiments, and Marv Leister for help with ^2H NMR measurements.

Note Added after ASAP Publication. An author's name was spelled incorrectly in the version of this paper published ASAP on September 19, 2006. The corrected version was published ASAP on September 20, 2006.

Supporting Information Available: A crystallographic information file (CIF) for (tpy')NiI₂. This material is available free of charge via the Internet at <http://pubs.acs.org>.

JA063334I